

Visibility graph approach to extreme event series

Jing Zhang(张晶), Xiaolu Chen(陈晓露), Haiying Wang(王海英), Changgui Gu(顾长贵), and Huijie Yang(杨会杰)
Citation: Chin. Phys. B, 2023, 32 (**10**): 100505. DOI: 10.1088/1674-1056/acd62b
Journal homepage: http://cpb.iphy.ac.cn; http://iopscience.iop.org/cpb

What follows is a list of articles you may be interested in

Sensitivity to external optical feedback of circular-side hexagonal resonator microcavity laser

Tong Zhao(赵彤), Zhi-Ru Shen(申志儒), Wen-Li Xie(谢文丽), Yan-Qiang Guo(郭龑强), An-Bang Wang(王安帮), and Yun-Cai Wang(王云才)
Chin. Phys. B, 2021, 30 (**12**): 120513. DOI: 10.1088/1674-1056/ac322a

Synchronization mechanism of clapping rhythms in mutual interacting individuals

Shi-Lan Su(苏世兰), Jing-Hua Xiao(肖井华), Wei-Qing Liu(刘维清), and Ye Wu(吴晔)
Chin. Phys. B, 2021, 30 (**1**): 010505. DOI: 10.1088/1674-1056/abb30a

Patterns of cross-correlation in time series: A case study of gait trails

Jia Song(宋佳), Tong-Feng Weng(翁同峰), Chang-Gui Gu(顾长贵), Hui-Jie Yang(杨会杰)
Chin. Phys. B, 2020, 29 (**8**): 080501. DOI: 10.1088/1674-1056/ab9287

Reconstruction of dynamic structures of experimental setups based on measurable experimental data only

Tian-Yu Chen(陈天宇), Yang Chen(陈阳), Hu-Jiang Yang(杨胡江), Jing-Hua Xiao(肖井华), Gang Hu(胡岗)
Chin. Phys. B, 2018, 27 (**3**): 030503. DOI: 10.1088/1674-1056/27/3/030503

A generalized model of TiO_x-based memristive devices andits application for image processing

Jiangwei Zhang(张江伟), Zhensen Tang(汤振森), Nuo Xu(许诺), Yao Wang(王耀), Honghui Sun(孙红辉), Zhiyuan Wang(王之元), Liang Fang(方粮)
Chin. Phys. B, 2017, 26 (**9**): 090502. DOI: 10.1088/1674-1056/26/9/090502

Visibility graph approach to extreme event series

Jing Zhang(张晶)[1,2], Xiaolu Chen(陈晓露)[1], Haiying Wang(王海英)[1], Changgui Gu(顾长贵)[1], and Huijie Yang(杨会杰)[1,†]

[1] *Department of Systems Science, University of Shanghai for Science and Technology, Shanghai* 200093, *China*
[2] *Department of Business, Wuxi Taihu University, Wuxi* 214064, *China*

(Received 25 March 2023; revised manuscript received 12 May 2023; accepted manuscript online 17 May 2023)

An extreme event may lead to serious disaster to a complex system. In an extreme event series there exist generally non-trivial patterns covering different time scales. Investigations on extreme events are currently based upon statistics, where the patterns are merged into averages. In this paper from extreme event series we constructed extreme value series and extreme interval series. And the visibility graph is then adopted to display the patterns formed by the increases/decreases of extreme value or interval faster/slower than the linear ones. For the fractional Brownian motions, the properties for the constructed networks are the persistence, threshold, and event-type-independent, *e.g.*, the degree distributions decay exponentially with almost identical speeds, the nodes cluster into modular structures with large and similar modularity degrees, and each specific network has a perfect hierarchical structure. For the volatilities of four stock markets (NSDQ, SZI, FTSE100, and HSI), the properties for the former three's networks are threshold- and market-independent. Comparing with the factional Brownian motions, their degree distributions decay exponentially but with slower speeds, their modularity behaviors are significant but with smaller modularity degrees. The fourth market behaves similar qualitatively but different quantitatively with the three markets. Interestingly, all the transition frequency networks share an identical backbone composed of nine edges and the linked graphlets. The universal behaviors give us a framework to describe extreme events from the viewpoint of network.

Keywords: extreme events, visibility graph

PACS: 05.45.Tp, 89.65.Gh **DOI:** 10.1088/1674-1056/acd62b

1. Introduction

Extreme events occur frequently in complex systems such as the global climate system and the stock markets over the world. The occurrence of an extreme event implies generally an unreasonable large deviation from the formal state, leading to serious damage to and even collapse of the system.[1]

A complex system is composed of many elements. Monitoring the dynamical process of the system produces a mono/multi-variate time series. Herein we adopt a simple definition of extreme event, namely, the value of a specific variable surmounts a threshold. From the time series for the interested variable, one finds the extreme events, each of which is composed of the value of the variable and the occurring time point. The successive values and the time intervals form the extreme value (EV) and the extreme interval (EI) series, called EV/EI-event type series, respectively.

Detailed works have been done on the behaviors of extreme events from the viewpoint of rare event statistics.[2] For example, starting from different initial distributions, there will appear three types of asymptotic distributions for maximum and minimum values, which are widely used in risk management, finance, material science, and so on. From the viewpoint of nonlinear dynamics, extreme events usually occur near the edges between different attractors. Accordingly, the unreasonable large of fluctuation and the significant strong of autocorrelation are widely used as early-warning signals for extreme events.[3–5] The extreme event series has generally short/long-term memory,[6–10] i.e., there exist nontrivial structures from microscopic to macroscopic scales. But these structures are lost in the procedure of statistics. Hence, displaying the non-trivial relation structures in extreme event series is a key step to understand extreme events.

Complex network theory is a natural tool to illustrate the relation structures in time series.[11,12] Network-based time series analysis is initially proposed by Zhang *et al.* in 2006.[13–15] From a pseudo-periodic time series, the periodic segments are extracted and taken to be nodes. For each pair of nodes, let the short one slide along the other and calculate the absolutes of the cross-correlation coefficients for the matched segments. If the largest one is larger than a specified threshold the two nodes are linked. An alternative strategy is to separate the time series into segments with a specified length, and calculate the distances between the segments. The segments are mapped to nodes and linked subsequently into a network by, *e.g.*, connecting only the pairs whose distances are less than a specified threshold,[16–20] filtering out some distant edges to be sure the resulting network can be embedded in a two-dimensional (2D) surface,[21] or linking each node with a

[†]Corresponding author. E-mail: hjyang@ustc.edu.cn

© 2023 Chinese Physical Society and IOP Publishing Ltd

specified number of its nearest nodes.[22]

People usually expect a linear increase/decrease of EV or EI. In the present work we take the linear increase/decrease as a reference, and are interested in the increases/decreases faster/slower than it. Accordingly, we adopt the visibility graph[23–26] to map the EV and EI series to networks. Technically, all the EVs/EIs are regarded as nodes. A pair of EVs/EIs is said to be visible each other only if a direct link between them has no intersection with the EVs/EIs between them. If two nodes are visible each other, we construct an edge between them. The resulting networks are called EV visibility graph and EI visibility graph, respectively. To our knowledge, our solution, i.e., converting the extreme event series into EI and EV series and mapping subsequently them into visibility graphs, is proposed by us for the first time.

We consider the fractional Brownian motions (fBm) with different Hurst exponents. The properties of the constructed visibility graphs are independent with the Hurst exponent, the threshold, and the event-type. The degree distributions decay exponentially with almost identical speeds. The nodes in the visibility graphs each cluster into high-modular structures with almost identical modularity degrees. In each visibility graph the communities at different scales are organized into a perfect hierarchical structure.

The volatilities of the indices for four stock markets distributed over the world are also considered. For the three markets of NSDQ, SZI, and FTSE100, the properties for the visibility graphs are event-type dependent. The degree distributions decay exponentially also, but the decaying speeds for the EV series and EI series are similar with and significantly smaller than that for the fBms, respectively. The modularity degrees are also very large, however, they are comparatively smaller and distribute in a wider range. The nodes in each visibility graph for the EV series are organized into a hierarchical structure, but the visibility graph for every EI series has not a hierarchical structure. The properties are threshold- and market-independent.

From each constructed visibility graph we extract all the linking patterns for series segments with a specified length, and reckon the successively occurring, i.e., transition frequencies for all the pairs of distinguishable patterns. Interestingly, in all the transition frequency networks for both the fBm and the stock market indices, there exists an identical backbone composed of nine edges and the linked patterns. The differences between the visibility graphs can be described with the weights of the edges.

These findings, especially the universal qualitative behaviors, may provide us a framework to understand and compare the extreme events from the viewpoint of complex network.

2. Methodology and materials

2.1. Materials

The fBm is used to generate extreme event series. An fBm is a continuous-time Gaussian process widely used to mimic the long-term correlations in empirical time series, such as the volatilities of stock markets.[27] Its increment series, $\{z(t,\tau) \equiv \mathrm{fBm}(t+\tau) - \mathrm{fBm}(t), t = 1,2,\ldots\}$, is stationary. The distribution function of the increments has a form of $\sim (1/\tau^H) F\left((z/\tau^H)\right)$, implying $\mathrm{var}[z(\tau)] \sim \tau^{2H}$, i.e., it has a scaling-invariant (persistent) behavior measured with the Hurst exponent $0 \leq H \leq 1$. Choosing $\tau = 1$ and $H \in [0.5, 1]$, one generates a increment series z, whose length should be large enough to be sure the extreme events (the values larger than the specified value of $\theta \in [1,3]$ in the normalized series of z) reaches a specified number of N.

In calculations, to make the results comparable with each other, we first generate a normalized series the number of the values bigger than a large threshold θ_0 (e.g., three times of the standard deviation) in which reaches N. And the extreme event series with $\theta < \theta_0$ are extracted simply from the generated extreme event series for $\theta = \theta_0$. The extreme event numbers are all chosen to be 2000. The generated EV and EI series are denoted as

$$\begin{aligned} Z^{\mathrm{ev}}(H,\theta) &\equiv \{z^{\mathrm{ev}}(H,\theta,m), m = 1,2,\ldots,2000\}, \\ Z^{\mathrm{ei}}(H,\theta) &\equiv \{z^{\mathrm{ei}}(H,\theta,m), m = 1,2,\ldots,1999\}, \end{aligned} \tag{1}$$

where $z^{\mathrm{ev}}(H,\theta,m)$ is the value for the m-th extreme event (the m-th EV), and $z^{\mathrm{ei}}(H,\theta,m)$ the time interval between the $(m+1)$-th and m-th extreme events (the m-th EI).

We consider also the daily closing price series for four stock markets distributed over the world, including the NSDQ from America, the SZI and HSI from China, and FTSE100 from British. The time duration starts from January 2004 and ends at June 2022, covering a period of 18 years, the lengths of which are ~ 4000. The original data are downloaded from the Website for Yahoo Finance.[28]

The volatility series are used. Denoting the closing price index series for a specific market with $\{p(t), t = 1,2,\ldots,T+1\}$, the corresponding volatility series reads

$$V = \left\{ \left| \log\left[\frac{p(k+1)}{p(k)}\right] \right|, \ t = 1,2,\ldots,T \right\}. \tag{2}$$

Let us denote the normalized series of V with v. The constructed EV and EI series from v read

$$\begin{aligned} v^{\mathrm{ev}}(\theta) &\equiv \{v^{\mathrm{ev}}(\theta,m), m = 1,2,\ldots,M\}, \\ v^{\mathrm{ei}}(\theta) &\equiv \{v^{\mathrm{ei}}(\theta,m), m = 1,2,\ldots,M-1\}, \end{aligned} \tag{3}$$

respectively. Here $v^{\rm ev}(\theta,m)$ is the value for the m-th extreme event (the m-th EV), and $v^{\rm ei}(\theta,m)$ the time interval between the $(m+1)$-th and m-th extreme events (the m-th EI), M the total number of extreme events.

2.2. Visibility graph

As an illustration, now we adopt the concept of visibility graph[23] to map the EV series $v^{\rm ev}(\theta)$ to a network. One maps the total of T entities in $v^{\rm ev}(\theta)$ as nodes numbered with $1,2,\ldots,T$, respectively. Two nodes are defined to be visible if they can "see" each other. Obviously, each pair of nearest neighbors are visible each other. For a pair of nodes separated by a total of $m>1$ nodes, e.g., the k-th and $(k+m+1)$-th nodes, their being visible each other implies that the straight line linking them is over all the m nodes between them. Mathematically it can be described with a set of inequalities

$$v^{\rm ev}(\theta,k)+\frac{v^{\rm ev}(\theta,k+m+1)-v^{\rm ev}(\theta,k)}{m+1}\times p\geq v^{\rm ev}(\theta,k+p),\quad p=1,2,\ldots,m. \tag{4}$$

Linking all the visible pairs of nodes results into a network, called EV visibility graph, represented with an adjacency matrix $A^{\rm ev}$ whose entity $A^{\rm ev}(i,j)$ equals (0) 1 when the nodes i and j are (dis-)connected.

One can understand the physical implication of the links in visibility graph from the viewpoint of prediction. If we link with straight lines the k-th node and the nodes numbered $k+1$, $k+2$, …, $k+m$, their slopes are all smaller than the one for the straight line between the k-th and the $(k+m+1)$-th node $[v^{\rm ev}(\theta,k+m+1)-v^{\rm ev}(\theta,k)]/(m+1)$. If we predict the value of the $(k+m+1)$-th node by extending the straight lines each, the predictions are all smaller than the real one. The predictions are called expected linear increases/decreases, and their being smaller than the real one is called the faster increase or slower decrease. The visibility graph is a realization of the idea "faster/slower than linear increase/decrease".

An analogous procedure can map the EI series $v^{\rm ei}(\theta)$ to a network, represented with adjacency matrix $A^{\rm ei}$ whose entity $A^{\rm ei}(i,j)$ equals (0) 1 when nodes i and j are (dis-)connected.

2.3. Network properties

Several properties, including the degree distribution, the community, the hierarchy, and transition between graphlets, are used to display the structural heterogeneities of constructed graphs from microscopic to macroscopic scales.[29]

(i) Degree distribution The degree of a node is the number of edges that connect directly this node with other nodes. In some networks the degrees distribute mainly in a sharp interval, i.e., the average of all the degrees is a good characteristic of the network. For instance, the degrees in an Erdos–Renyi network obeys a Poisson distribution characterized by the mean degree. For some other networks, the degrees distribute in wide ranges, i.e., there exists not a specific degree taking as characteristic. A typical example is the scale-free network, in which the degree distribution obeys a power-law. Theoretical analysis shows that the visibility graph algorithm maps the fBm increment series to a scale-free network, the decaying exponent for which is determined by the the Hurst exponent H.[25,30] Degree distribution is a measure of microscopic heterogeneity at the individual node scale.

(ii) Community Generally speaking, in a network the nodes cluster into different dense communities, i.e., within each community the nodes are tightly connected with edges, and between the communities there exist few edges. Extensive works have been devoted to the detection of communities, among which the Newman–Girvan algorithm[31,32] is widely accepted, where a quantity $Q\in[0,1]$ is defined to measure the modularity degree. A larger Q implies a higher modular behavior. Obviously, Q is a measure of macroscopic heterogeneity at the global level.

(iii) Hierarchy Clustering coefficient for a specific node k, denoted with C_k, is the ratio of the existing number over the possible number of edges between its neighbors, describing the probability of its neighbors' being connected. In many empirical networks, the average of the clustering coefficients for the nodes with identical degrees obeys a power-law with respect to the degree, i.e., $\langle C(d)\rangle\sim d^{-\gamma}$, where d is degree. The scaling exponent γ is network structure-dependent. Analytical and numerical works show that if the network has a hierarchical structure, i.e., the communities can be divided into sub-communities iteratively, and the sub-communities at smaller scales are organized into the ones at larger scales with identical laws, the scaling exponent is unity, $\gamma=1$.[33]

In this work, this power-law is used to detect the hierarchical behavior of the constructed visibility graphs. For instance, for the k-th node in the graph $A^{\rm ev}$, its clustering coefficient reads,

$$C_k^{\rm ev}=\frac{[A^{\rm ev}\cdot A^{\rm ev}\cdot A^{\rm ev}]_{kk}}{D(k)\cdot[D(k)-1]},$$

where $D(k)=[A^{\rm ev}\cdot A^{\rm ev}]_{kk}$ is the degree of the node k. If we have the relation of $\langle C^{\rm ev}(d)\rangle\sim d^{-\gamma}$, we conclude that the visibility graph is built from the microscopic to the macroscopic structure in a hierarchical way.

(iv) Graph-lets Let a window with a specified length w slide along the EV/EI series, the visibility graphs for the covered series segments are called graph-lets, representing the states of the system in the corresponding time durations.[34–43] The successive graph-lets gives us the evolutionary trajectory

of the system. One enumerates all the possible distinguishable graph-lets and give them each identification numbers such as $1,2,\ldots,G$, forming a graph-let dictionary. From the pairs of visibility graph-lets corresponding to successive series segments, we obtain the pattern transition frequency matrix, $A^{\rm freq}$, the entity $A^{\rm freq}(m,n)$ $(m,n=1,2,\ldots,G)$ of which is the occurring frequency of the jump from the present n-th graph-let to the next m-th one. By this way all the possible graph-lets are linked by the transition frequencies between them into a transition frequency network, represented with the adjacency matrix $A^{\rm freq}$. The edges with significantly large frequencies and the graph-lets linked by them form the structural backbone.

Herein, for each node in the transition frequency network, we are specially interested in its out-weight-degree $d^{\rm W}(\cdot)$ and out-entropy-degree $d^{\rm E}(\cdot)$, which read,

$$d^{\rm W}(n)=\sum_{m=1}^{G}A^{\rm freq}(m,n),$$
$$d^{\rm E}(n)=-\frac{1}{\ln G}\sum_{m=1}^{G}\frac{A^{\rm freq}(m,n)}{\sum_{i=1}^{G}A^{\rm freq}(i,n)}\ln\left[\frac{A^{\rm freq}(m,n)}{\sum_{i=1}^{G}A^{\rm freq}(i,n)}\right],$$
$$n=1,2,\ldots,G. \tag{5}$$

The former tells us the times of transitions from the interested graph-let to the other ones (including itself), and the later the concentration behavior of the transitions. A smaller $d^{\rm E}(\cdot)$ implies the transition concentrates on fewer destinations, i.e., the transition is much more predictable.

3. Results

3.1. Constructed EI and EV series

For the fBm, the threshold θ is chosen to be $1.0+0.1\times(\kappa-1),\kappa=1,2,\ldots,21$, i.e., $\theta\in[1,3]$, to construct the extreme events, shown in Fig. 1 are typical examples of EI series (panels Figs. 1(a1)–1(b1)) and EV series (panels (c1)–(d1) for $H=0.65$ and $H=0.75$ with $\theta=1.0$, 1.5, 2.0, 2.5, and 3.0, respectively. For the stock market volatility series, the threshold θ is chosen to be 0.5 and 1.0, to be sure the number of constructed extreme events is large enough for statistics, the EI and EV series corresponding to which are displayed in the panels (a2)–(b2) and (c2)–(d2), respectively. The series behave clustering, i.e., bigger/smaller values tend to cluster together, forming fluctuation peaks/valleys.

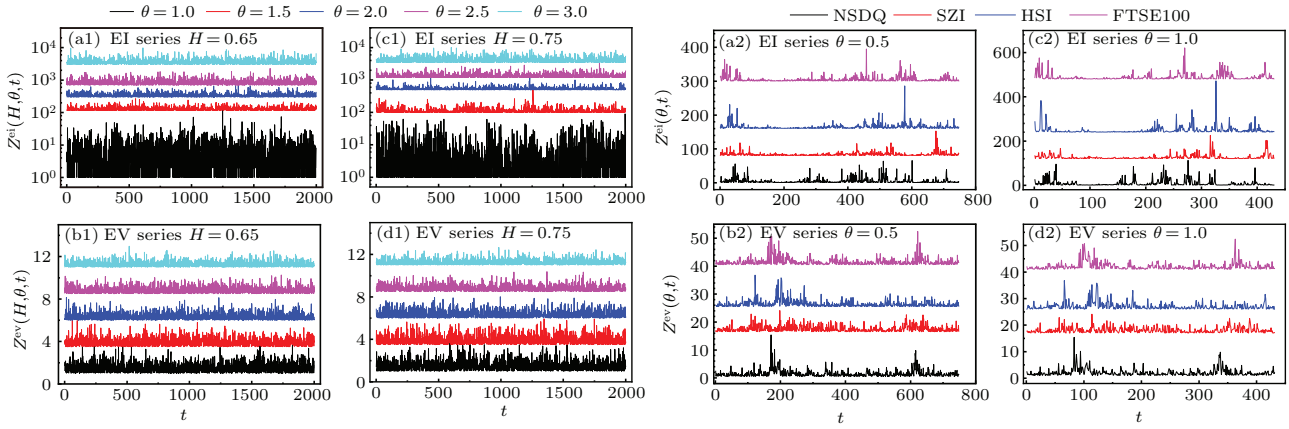


Fig. 1. Constructed EI and EV series. (a1)–(b1) and (c1)–(d1) The EI and EV series constructed from fBm with $H=0.65$ and $H=0.75$, respectively; $\theta=1.0$, 1.5, 2.0, 2.5, 3.0. For EI series, the log-scale is used for visual convenience. (a2)–(b2) and (c2)–(d2) The EI and EV series constructed from the stock market volatility series with $\theta=0.5$, 1.0 [(c2)–(d2)], respectively. The curves are shifted vertically for visual convenience.

3.2. Degree distributions

Figure 2 presents the degree distributions for all the constructed EI series (panels (a1)–(a3)) and EV series (panels (b1)–(b3)) generated by the fBm with $H=0.65,0.75$, and 0.85. When the degree is large enough (>7) the curves all decay exponentially in a wide range of degree d, i.e., $\sim\exp(-\alpha d)$. The decaying exponents for the EI and EV series fall in the ranges of $[0.18,0.23]$ and $[0.19,0.24]$, whose means and standard deviations read 0.20 ± 0.018 and 0.22 ± 0.016, respectively. They are also very close with each other, being independent with H,θ and EI/EV-event type.

For the EI and EV series constructed from the stock volatility series, the degree distributions decay exponentially also. All the decaying exponents for the EI series (panels (c1)–(d1)) are very close with each other (0.16 ± 0.01), except the smaller one for the HSI with $\theta=1$ ($\alpha=0.12$). All the decaying exponents for the EV series (panels (c2)–(d2)) are almost identical ($\alpha=0.22\pm0.01$), except the smaller one for HSI with $\theta=1$ ($\alpha=0.17$). The corresponding shuffled series are also generated, as shown in the panels (d1)–(d2) two typical results for the NSDQ with $\theta=1.0$ (the open circles), whose decaying exponents turn out to be significantly different with that for the original series.

Hence, except that for the HSI, the decaying behavior for each specific EI/EV-event type degree distribution is independent of the threshold θ and the market.

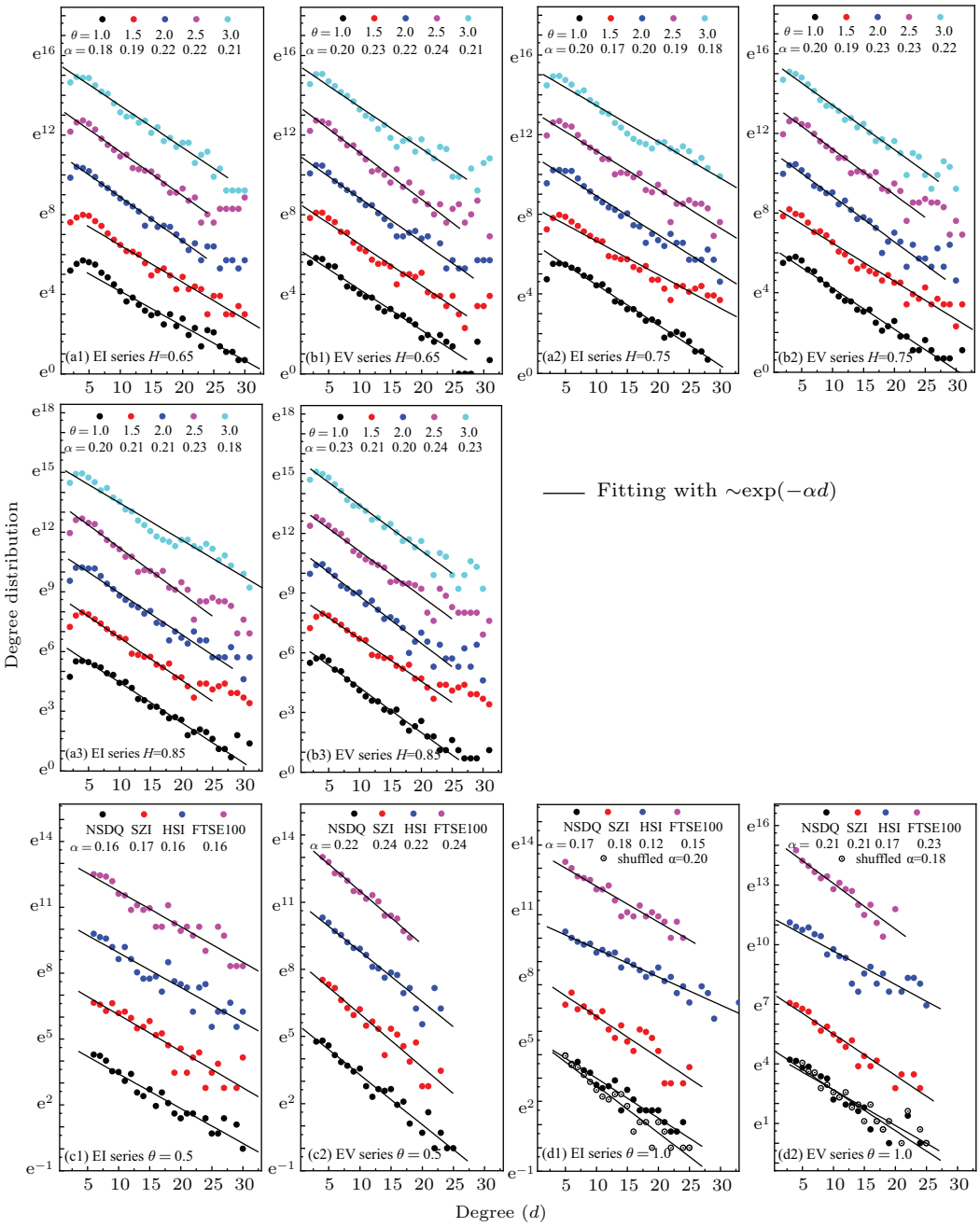


Fig. 2. Degree distributions for the constructed visibility graphs. (a1)–(a3) The EI series constructed from fBm. $H = 0.65$, 0.75, 0.85 and $\theta = 1.0$, 1.5, 2.0, 2.5, 3.0. (b1)–(b3) The EV series constructed from fBm. $H = 0.65$, 0.75, 0.85 and $\theta = 1.0$, 1.5, 2.0, 2.5, 3.0. (c1)–(d1) The EI series constructed from the stock volatility series. $\theta = 0.5$, 1.0. (c2)–(d2) The EV series constructed from the stock volatility series. $\theta = 0.5$, 1.0. The curves are shifted vertically for visual convenience, which does not impact the estimation of the decaying exponents. Open circles are the results for shuffled EI and EV series. The least-square regression is adopted to estimate the slopes. In the shuffled series the elements are positioned in a completely random order.

3.3. Modularity and hierarchy

Figure 3 provides the modularity Q for all the constructed visibility graphs. The values of Q for the EI series (panel (a1)) and the EV series (panel (a2)) constructed from fBm fall in the ranges of $[0.82, 0.88]$ and $[0.83, 0.86]$, respectively.

From the Q values for the EI and EV series constructed from the stock volatility series (panel (b1)) one can find that, comparatively for each specific market and threshold θ, the Q for the EV series is significantly larger than that for the EI series. For each specific market and EI/EV-event type, the larger value of $\theta = 1$ implies a smaller value of Q. The Q value for the EI series of HSI decreases from 0.72 to 0.54 with the increase of θ from 0.5 to 1.0, the difference between which is significantly larger compared with that for the other markets. The values of Q for all the visibility graphs except the anomalous one of 0.54 are in the interval of $[0.66, 0.81]$, i.e., the visibility graphs each are composed of significant modular structures. Panel (b2) gives the modularity values for the corresponding shuffled series, which are comparatively larger but close with each other and undistinguishable with that for the fBm series.

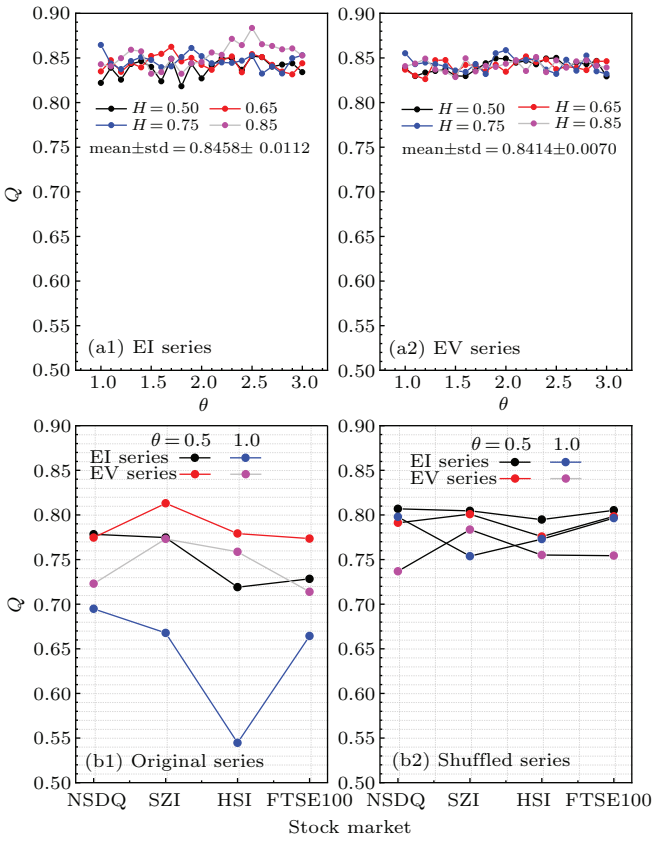


Fig. 3. Modularity degrees Q for the visibility graphs. (a1)–(a2) The EI and EV series constructed from fBm. (b1) The EI and EV series constructed from stock volatility series. (b2) The shuffled EI and EV series constructed from stock volatility series.

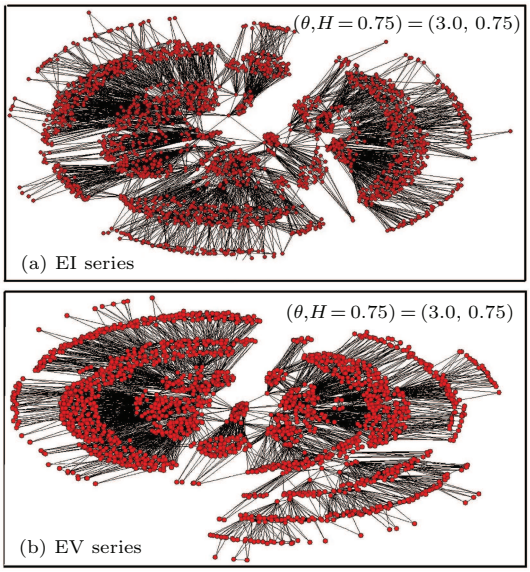


Fig. 4. Two examples of visibility graphs for EI series (a) and EV series (b) constructed from fBm. $H = 0.75$, $\theta = 3.0$. The strategy of node repulsion and equal length bias is adopted to realize the layouts.

Figure 4 provides the topological structures for the EI series (panel (a)) and the EV series (panel (b)) constructed from fBm with $(\theta, H) = (3.0, 0.75)$. The networks each are composed of non-overlapping communities, and they each are composed of distinguishable sub-communities, and the sub-communities the sub-sub-communities, resulting into several levels of modular structures. The topological structures for the EI and EV series for the four stock markets with $\theta = 1$ are shown in Fig. 5. The layouts of the nodes are realized by using the strategy of node repulsion and equal length bias.

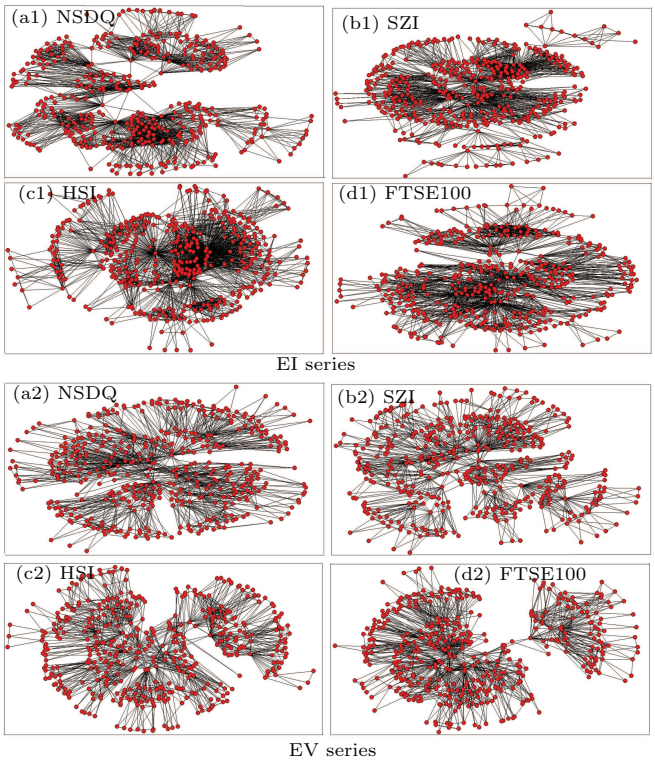


Fig. 5. Visibility graphs for EI series [(a1)–(d1)] and EV series [(a2)–(d2)] constructed from the stock volatility series. $\theta = 1.0$. The strategy of node repulsion and equal length bias is adopted to realize the layouts.

These findings are consistent with the scaling behaviors in the relations of average of clustering coefficients for the nodes with identical degrees versus degree, as shown in Fig. 6. For the EI series (panels (a1)–(a3)) and the EV series (panels (b1)–(b3)) constructed from fBm, when the degree is larger than 7 the curves $\langle C^{\rm ei}(d)\rangle$ and $\langle C^{\rm ev}(d)\rangle$ versus the degree d all satisfy power-laws with scale-invariant exponents of $\gamma \in [0.85, 1.09]$, whose mean and standard deviation read 0.97 ± 0.06. Hence, the networks have almost perfect hierarchical structures.

For the EI series constructed from the stock volatility series (panels (c1)–(d1)), the curves decay exponentially with different exponent values, being different with the power-laws for the fBm series. The corresponding visibility graphs have subsequently not hierarchical structures. For the EV series constructed from the stock volatility series (panels (c2)–(d2)), the curves each (when $d \geq 5$), obey perfect power-laws. The values of the scaling exponents read $\gamma = 0.86 \pm 0.05$, being significantly smaller than that for the fBm series (0.97 ± 0.06), implying that the visibility graphs have hierarchical structures but not perfect as that for the corresponding fBm series. The corresponding shuffled series have different behaviors, e.g., the relation for the shuffled EI series constructed from the NSDQ volatility series (the circles in panel (d1)) obeys a power-law rather than an exponential one.

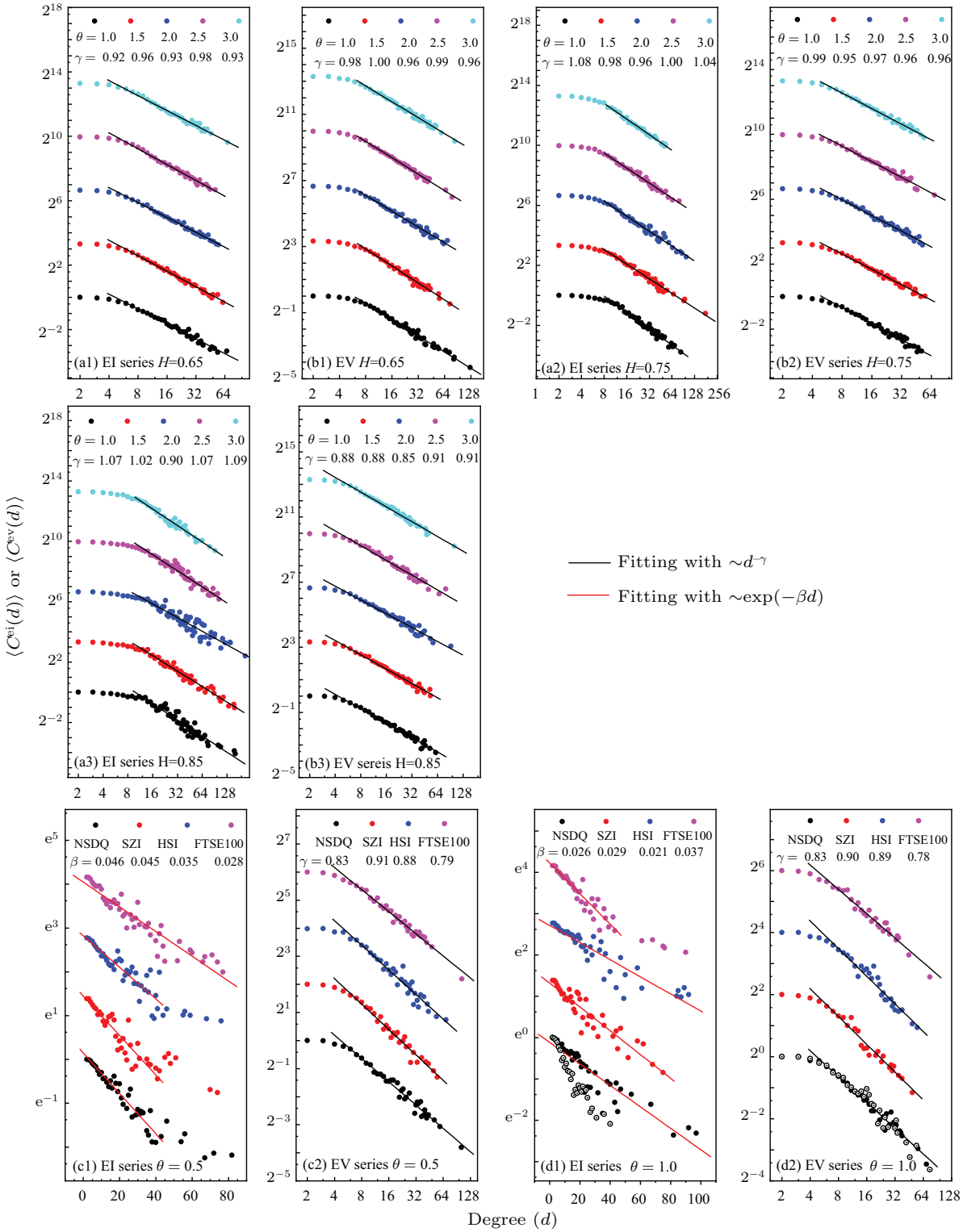


Fig. 6. The average of clustering coefficients for the nodes with identical degrees. (a1)–(a3) the EI series and (b1)–(b3) the EV series constructed from fBm. $\theta = 1.0$, 1.5, 2.0, 2.5, 3.0, $H = 0.65$, 0.75, and 0.85. (c1)–(d1) the EI series and (c2)–(d2) the EV series constructed from the stock volatility series. $\theta = 0.5$, 1.0. The curves are shifted vertically for visual convenience. The circles in panels (d1) and (d2) are the results for the shuffled EI and EV series for the NSDQ market. The least-square regression is adopted to estimate the slopes. In the shuffled series the elements are positioned in a completely random order.

3.4. Transitions between graphlets: A universal backbone

Figure 7 gives the average frequencies of transitions between the visibility graph-lets. The length of the series segments is chosen to be $w = 5$, corresponding to which there are totally $G = 25$ distinguishable graph-lets, numbered 1 to 25.[44] The pattern transition frequency matrix A^{freq} is composed of $25 \times 25 = 625$ edges. Herein each edge is re-assigned a new identification number, called edge ID. The reassigning rule is, $(i, j) \longrightarrow (j-1) \cdot 25 + i$, i.e., the edge from j to i is renumbered with $(j-1) \cdot 25 + i$.

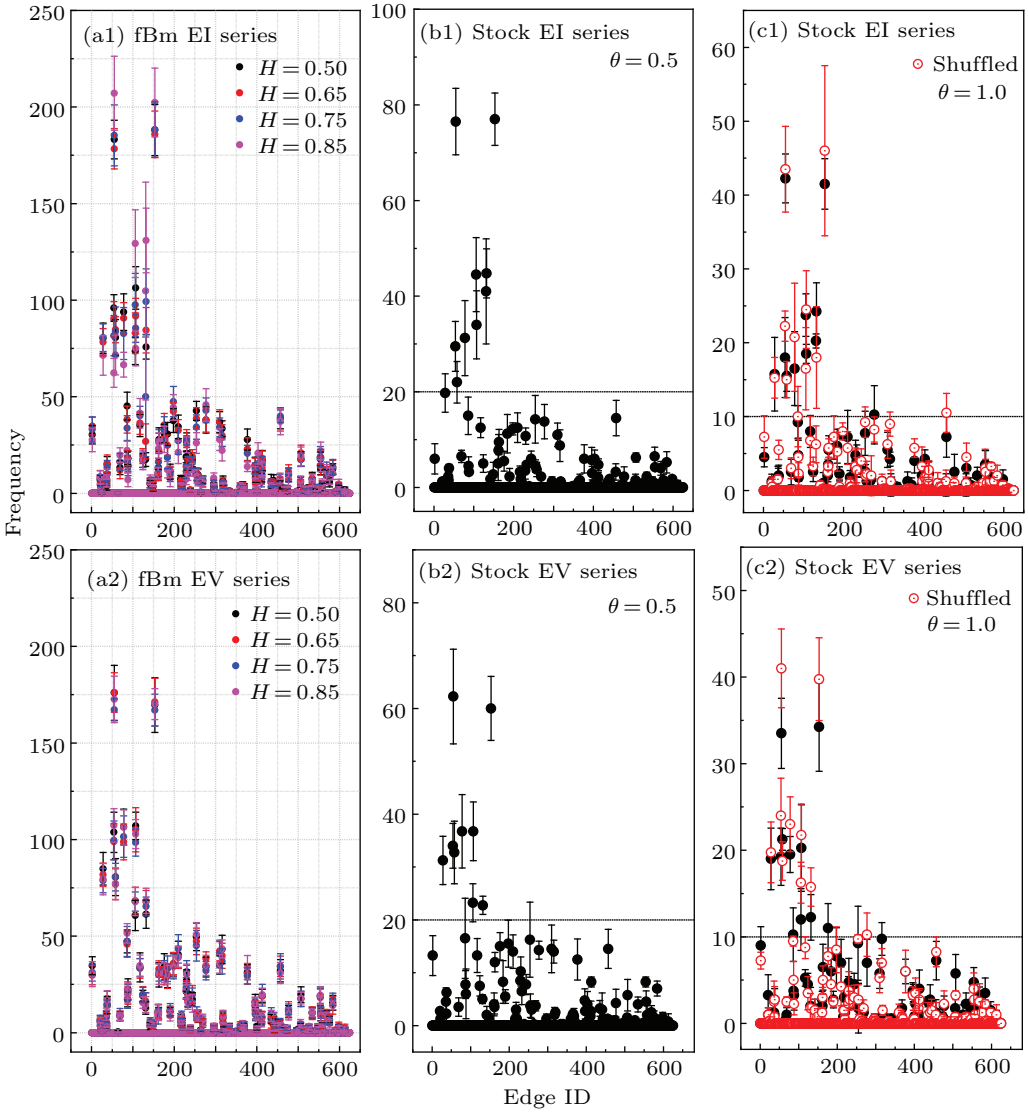


Fig. 7. The average frequencies of transitions between graph-lets. The transition from the j-th graphlet to the i-th graph-let is assigned an identification number (edge ID) of $(j-1)\cdot 25+i$. (a1)–(a2) the EI series and the EV series constructed from fBm. $\theta = 1.0, 1.1, \ldots, 3.0$. Panels (b1)–(b2) and (c1)–(c2) are the EI series and the EV series constructed from the stock volatility series, with $\theta = 0.5$ and 1.0, respectively. The red open circles are the results for the shuffled extreme series. In the shuffled series the elements are positioned in a completely random order.

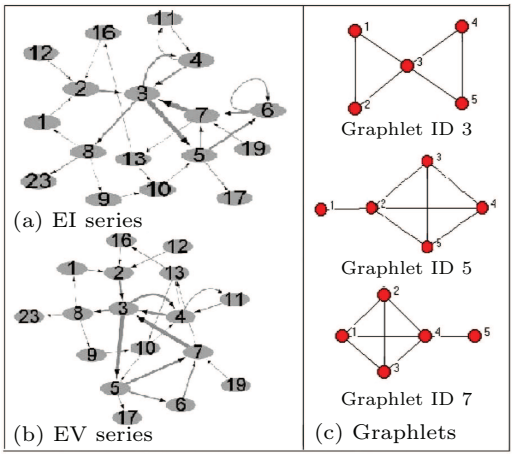


Fig. 8. The average transition frequency networks for the EI series (a) and the EV series (b) constructed from fBm. In panel (a) the backbone is composed of the bidirectional transition $3 \leftrightarrow 4$ and the loop $3 \longrightarrow 5 \longrightarrow 6 \longrightarrow 7 \longrightarrow 3$. In panel (b) the backbone is composed of the bidirectional transition $3 \leftrightarrow 4$ and the loop $3 \longrightarrow 5 \longrightarrow 7 \longrightarrow 3$. (c) The topological structures for the graph-lets with IDs 3, 5, and 7. The visibility graphs for the EI and EV series constructed from the stock volatility series have an identical backbone.

For the EI and EV series constructed from fBm, the average and standard deviation for each specific edge are obtained from the totally 21 networks corresponding $\theta = 1.0, 1.1, 1.2, \ldots, 3.0$. The averages for the cases with different H are close with each other, and the standard deviations are all small, resulting sharp confidence regions (panels (a1)–(a2) in Fig. 7), i.e., the transition frequency for each edge is weakly dependent with the Hurst exponent H and the threshold θ. Accordingly, in Fig. 8 we draw only the average transition frequency networks for the EI series (panel (a)) and the EV series (panel (b) in Fig. 8). Some transitions with high frequencies form a backbone. For example, the backbone in panel (a) is composed of the bidirectional transition of $3 \leftrightarrow 4$ and the loop of $3 \longrightarrow 5 \longrightarrow 6 \longrightarrow 7 \longrightarrow 3$, and that in panel (b) the bidirectional transition of $3 \leftrightarrow 4$ and the loop of $3 \longrightarrow 5 \longrightarrow 7 \longrightarrow 3$. The structures for the graph-lets numbered 3, 5, and 7 are also displayed in Fig. 8(c).

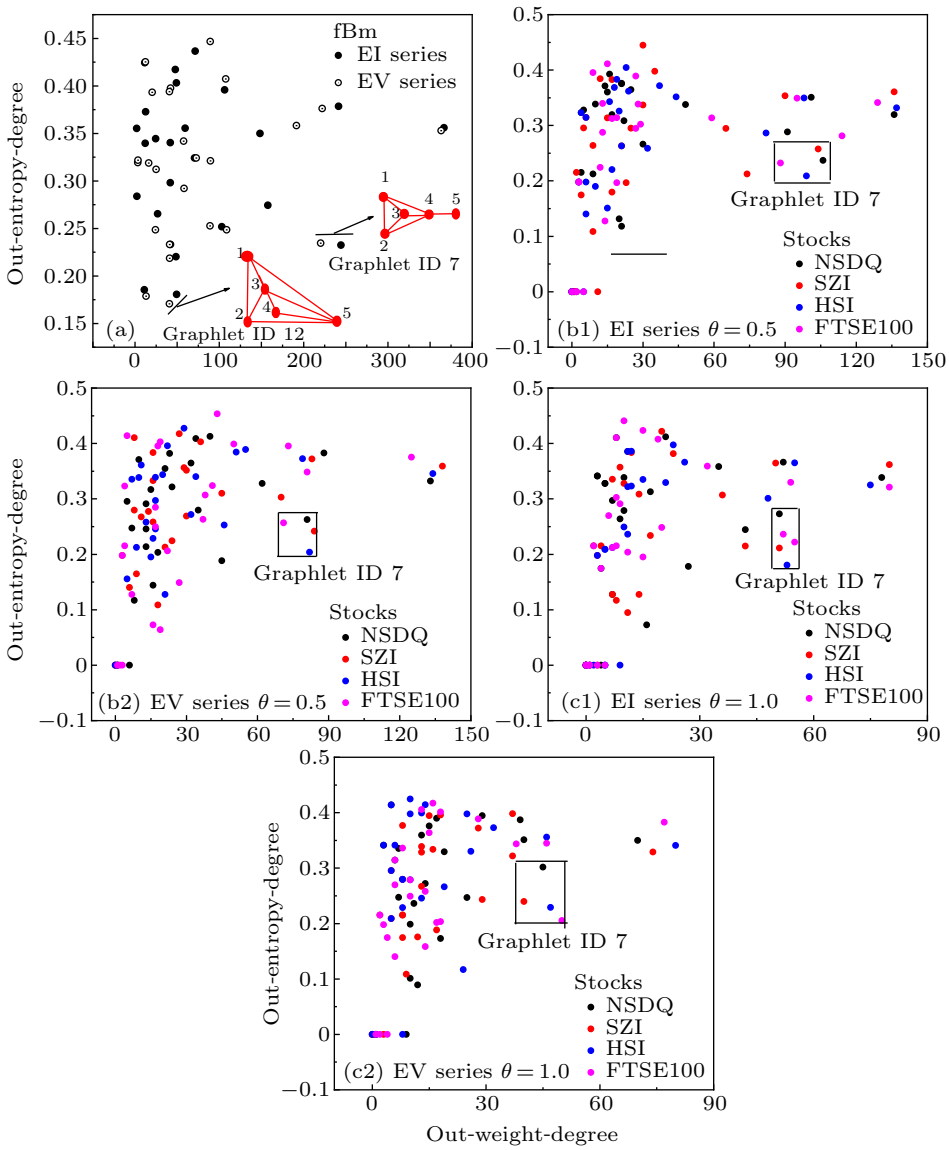


Fig. 9. The relation of out-entropy-degree versus out-weight-degree. (a) EI and EV series constructed from fBm. (b1)–(c1) EI series and (b2)–(c2) series constructed from the stock volatility series with $\theta = 0.5$ and 1.0, respectively. The graph-let numbered 7 has the large out-weight-degree and the small out-entropy degree. Once it occurs, we can predict confidently the following pattern. Its structure is depicted in panel (a).

For the EI and EV series constructed from the stock volatility series, the average and standard deviation for each specific edge are obtained from the four networks corresponding to each specified θ and Ei/EV-event type. As shown in panels (b1)–(b2) and (c1)–(c2) in Fig. 7, each average edge has a sharp confidence region, i.e., it is weakly dependent with the market. If we select the thresholds for the cases of $\theta = 0.5$ and 1.0 to be 10 and 20 (about unitary standard deviations larger than the averages) respectively, the backbones for the totally 16 transition frequency networks (not shown) share a pattern formed by seven edges, $4 \longleftrightarrow 3 \longrightarrow 5 \longrightarrow 7 \longrightarrow 3 \longrightarrow 8 \longleftarrow 2$. In the eight transition frequency networks for the EI series, two additional linkages join in this pattern, i.e., $5 \longrightarrow 6 \longrightarrow 6 \longrightarrow 7$, forming an extended pattern (not shown). A simple comparison with the patterns displayed in Fig. 8 shows that the topological structure for the extended pattern is identical with that for the corresponding backbone for the fBms. Hence, this backbone pattern spans a topological space, in which a specific transition frequency network can be represented with the weights of edges on the pattern. A simple comparison of the results for the shuffled extreme series (red open circles and the bars in panels (c1)–(c2) in Fig. 7) with that for the original extreme series shows that, the shuffling procedure does not destroy the backbone but the weights are significantly different.

The scatter diagrams for out-entropy degree versus out-weight degree are presented in Fig. 9. Most of the out-entropy degrees for all the graph-lets are all significantly smaller than that for the homogenously transition case, i.e., $\max(d^{\mathrm{E}}(n), n = 1, 2, \ldots, 25) = 0.45 \ll 1.0$ (see panel (a) for the EI and EV series constructed from fBm, and panels (b1)–(b2) and (c1)–(c2) in Fig. 9 for that from the stock volatility series). And the graph-let numbered 7 has a small value of $d^{\mathrm{E}}(7)$ and a large value of $d^{\mathrm{W}}(7)$, i.e., it occurs in the series with a high

frequency, and once it occurs one can predict the following local pattern of the time series. The topological structure for it and that numbered 12 are drawn (red graph-lets). The transition 7 $\longrightarrow$ 3 in the backbone pattern occurs with significantly higher probability.

4. Conclusion

A series of extreme events stores rich patterns that can not only shed light on the underlying event's occurring mechanism, but also help us in management of risks in the complex system. The approaches in literatures are currently based upon the theory of statistics. Most of the patterns and their relationships are lost in the shared procedure of statistical average. In the present work, by using the concept of visibility graph we investigate the patterns formed by the increases/decreases of extreme event size faster/slower than the linear ones.

For the extreme event series extracted from fBm series, the properties of the corresponding visibility graphs are independent with the persistent behavior (measured with the Hurst exponent H), the threshold θ, and the EI/EV-event-type. For instance, the degree distributions decay exponentially with almost identical exponents (0.20 ± 0.016). The visibility graphs all have high modular behaviors ($Q = 0.83 \pm 0.03$). In each visibility graph, the communities at different scales are organized into a perfect hierarchical structure.

For the extreme event series extracted from the volatility series of three stock market indices (NSDQ, SZI, and FTSE100), the degree distributions decay also exponentially, the decaying speeds for which are however EI/EV-event-type dependent, i.e., the exponents for the EI and EV series fall in 0.16 ± 0.01 and 0.22 ± 0.01, respectively. The modularity degrees Q are in a wider range of 0.74 ± 0.08 compared with that for the fBms. The communities for each EV series are also organized into a hierarchical structure, but the values of γ fall in 0.86 ± 0.05, significantly smaller than that in fBms ($0.97 \pm 0.06 \sim 1.0$), i.e., the hierarchical behavior is significantly weak compared with that for the fBms. The communities for the EI series are not organized into hierarchical structures. Hence, the topological structures for the empirical records are event-type dependent, and threshold and market independent.

Interestingly, all the transition frequency networks for the fBm and the stock market indices share an identical backbone composed of nine edges and the linked graphlets, i.e., $4 \longleftrightarrow 3 \longrightarrow 5 \longrightarrow 6 \longrightarrow 6 \longrightarrow 7 \longrightarrow 3 \longrightarrow 8 \longleftarrow 2$. They span a topological space, in which each transition frequency network can be coordinated by using its specific weights for the nine edges.

Comparing with the statistics based methods, the visibility graphs (complex networks) mapped from time series can preserve and show us the details of the structures, especially the high-order structures in time series. The EI and EV series constructed from the fBm series with different long-term memories (measured by the Hurst exponent H) share the universal characteristics for the structural properties. This fact tell us that the difference in the long-term memory behaviors leads not significant changes to the high-order structures. A large amount of empirical investigations show us that the stock market volatility series have long-range correlations. The EI and EV series constructed from the stock market volatility series expose rich characteristics for the structural properties compared with that from the fBm series. This finding tells us that besides the persistent behavior shared with the fBm series, the volatility series have some new high-order structures. Deep understanding of the characteristics needs detailed works on a large amount of data in future works.

Acknowledgements

Project supported by the National Natural Science Foundation of China (Grant Nos. 11805128, 11875042, and 11505114) and the Shanghai Project for Construction of Top Disciplines, China (Grant No. USST-SYSBIO).

References

[1] Chowdhurya S N, Ray A, Dana S K and Ghosh D 2022 *Phys. Rep.* **966** 1
[2] Majumdar S N, Pal A and Schehr F 2020 *Phys. Rep.* **840** 1
[3] Scheffer M, Bascompte J, Brock W A, Brovkin V, Carpenter S R, *et al*. 2009 *Nature* **461** 53
[4] Battiston S, Farmer J D, Flache A, Garlaschelli D, Haldane A G, Heesterbee K H, *et al*. 2016 *Science* **351** 818
[5] Arani B M S, Carpenter S R, Lahti L, Nes E H V and Scheffer M 2021 *Science* **372** eaay4895
[6] Bunde A, Eichner J F, Kantelhardt J W and Havlin S 2005 *Phys. Rev. Lett.* **94** 048701
[7] Bunde A, Eichner J F, Kantelhardt J W and Havlin S 2006 *Phys. Rev. E* **73** 016130
[8] Santhanam M S and Kantz H 2008 *Phys. Rev. E* **78** 051113
[9] Nicolis C and Nicolis G 2009 *Phys. Rev. E* **80** 061119
[10] Aghamohammadi C and Crutchfield J P 2017 *Phys. Rev. E* **95** 032101
[11] Gao Z K, Small M and Kurths J 2016 *Europhys. Lett.* **116** 50001
[12] Zou Y, Donner R V, Marwan N, Donges J F and Kurths J 2019 *Phys. Rep.* **787** 1
[13] Zhang J and Small M 2006 *Phys. Rev. Lett.* **96** 238701
[14] Zhang J, Luo X, Nakamura T, Sun J and Small M 2007 *Phys. Rev. E* **75** 016218
[15] Zhang J, Sun J, Luo X, Zhang K, Nakamura T and Small M 2008 *Physica D* **237** 2856
[16] Yang Y and Yang H J 2008 *Physica A* **387** 1381
[17] Marwan M, Donges J F, Zou Y, Donner R V and Kurths J 2009 *Phys. Lett. A* **373** 4246
[18] Donner R, Zou Y, Donges J, Marwan N and Kurths J 2010 *New J. Phys.* **12** 033025
[19] Gao Z and Jin N D 2009 *Phys. Rev. E* **79** 066303
[20] Pham T D 2017 *Europhys. Lett.* **118** 20003
[21] Tumminello M, Aste T, Matteo T D and Mantegna R N 2005 *Proc. Natl. Acad. Sci. USA* **102** 10421
[22] Xu X, Zhang and Small M 2008 *Proc. Natl. Acad. Sci. USA* **105** 19601
[23] Lacasa L, Luque B, Ballesteros F, Luque J and Nuno C 2008 *Proc. Natl. Acad. Sci. USA* **105** 4972
[24] Luque B, Lacasa L, Ballesteros F and Luque J 2009 *Phys. Rev. E* **80** 046103
[25] Ni X H, Jiang Z Q and Zhou W X 2009 *Phys. Lett. A* **373** 3822

[26] Xiao Q, Pan X, Li X L, Mutua S, Yang H J, Jiang Y, Wang J Y and Zhang Q J 2014 *Chin. Phys. B* **23** 078904
[27] Mantegna R N and Stanley H E 2000 *Introduction to Econophysics: Correlations Complexity in Finance* (Cambridge University Press, Cambridge)
[28] https://uk.finance.yahoo.com/world-indices/ Accessed in July 20, 2022
[29] Albert R and Barabasi A L 2002 *Rev. Mod. Phys.* **74** 47
[30] Lacasa L, Luque L, Luque B and Nuno J C 2009 *Europhys. Lett.* **86** 30001
[31] Girvan M and Newman M E J 2002 *Proc. Natl. Acad. Sci. USA* **99** 7821
[32] Newman M E J and Girvan M 2004 *Phys. Rev. E* **69** 026113
[33] Ravasz E and Barabasi A L 2003 *Phys. Rev. E* **67** 026112
[34] McCullough M, Small M, Stemler T and Iu H C 2015 *Chaos* **25** 053101
[35] Stephen M, Gu C G and Yang H J 2015 *PLoS ONE* **10** e0143015
[36] Iacovacci J and Lacasa L 2016 *Phys. Rev. E* **93** 042309
[37] Mutua S, Gu C G and Yang H J 2016 *Chaos* **26** 053107
[38] Kulp C W, Chobot J M, Freitas H R and Sprechini G D 2016 *Chaos* **26** 073114
[39] McCullough M, Small M, Iu H H C and Stemler T 2017 *Phil. Trans. Roy. Soc. A* **375** 20170016
[40] McCullough M, Sakellariou K, Stemler T and Small M 2017 *Chaos* **27** 035814
[41] Zhang J Y, Zhou J, Tang M, Guo H, Small M and Zou Y 2017 *Sci. Rep.* **7** 7795
[42] Guo H, Zhang J Y, Zou Y and Guan S G 2018 *Front. Phys.* **13** 130508
[43] Ren H G, Yuan Q S, Semba S, Weng T F, Gu C G and Yang H J 2020 *Phys. Lett. A* **384** 126781
[44] Wang Y, Weng T F, Deng S G, Gu C G and Yang H J 2019 *Chaos* **29** 023109